AMERICAN ACADEMY OF OPHTHALMOLOGY®

Gaze-Evoked Deformations in Optic Nerve Head Drusen

Repetitive Shearing as a Potential Factor in the Visual and Vascular Complications

Patrick A. Sibony, MD,[1] Junchao Wei, PhD,[2] Ian A. Sigal, PhD[2,3]

Purpose: To determine if ocular ductions deform intrapapillary and peripapillary tissues in optic nerve head drusen (ONHD) and to compare these deformations with healthy eyes and eyes with other optic neuropathies.

Design: Observational case series.

Participants: Twenty patients with ONHD.

Methods: Axial rasters of the optic nerve from a spectral-domain OCT device (Cirrus 5000; Carl Zeiss Meditec, Inc, Dublin, CA) were used to analyze the shape of the peripapillary basement membrane (ppBM) layer in 20 confirmed cases of ONHD. We compared registered images obtained from 2 eye positions: 10° to 15° in adduction and 30° to 40° in abduction. Geometric morphometrics was used to analyze the shape of the ppBM layer defined by placing 10 equidistant landmarks extending 2500 μm on both sides of the basement membrane opening. We also adapted an image strain tracking technique to measure regional intrapapillary strains in 6 patients. Using manually placed nodes on the reference image (in adduction), an iterative, block-matching algorithm is used to determine local displacements between the reference and its paired image in abduction. Displacement vectors were used to calculate the mean shear and effective strain (percent change).

Main Outcome Measures: Peripapillary shape deformations, intrapapillary shear strains, and effective strains.

Results: We found a statistically significant difference in the shape of the ppBM layer between abduction and adduction ($P < 0.01$). The deformation was characterized by a relative posterior displacement temporally in adduction that reversed in abduction. Strain tracking in all 6 patients showed substantial gaze-induced shearing and effective strains. Mean effective strains were 7.5% outside the drusen. Shear and effective strains were significantly larger outside versus within the drusen ($P < 0.003$ and $P < 0.01$, respectively).

Conclusions: This study demonstrates that horizontal ocular ductions induce significant shearing deformations of the peripapillary retina and prelaminar intrapapillary tissues. We also found that the deformations in healthy persons are similar in magnitude to ONHD. Based on these findings, we speculate that patients with intrapapillary calcifications exposed to the long-term effects of repetitive shearing (induced by ocular ductions) may contribute to the progressive axonal loss and vascular complications associated with ONHD. *Ophthalmology 2017;■:1–9 © 2017 by the American Academy of Ophthalmology*

Supplemental material available at www.aaojournal.org.

Pseudopapilledema with optic nerve head drusen (ONHD) are intrapapillary calcifications that range in size between 5 and 1000 μm. Early on, buried deep within the prelaminar optic nerve head (ONH), they may not be seen ophthalmoscopically but gradually will become visible as they enlarge and approach the surface. The associated elevation and blurring of the disc can be confused with papilledema. Optic nerve head drusen are associated with a slowly progressive loss of peripheral vision and, rarely, acute vision loss resulting from neuroretinal vascular complications.[1–6]

Using spectral-domain OCT, we and others recently have shown that horizontal ocular ductions induce deformations of the ONH and peripapillary tissues in healthy participants,[7–9] in those with anterior ischemic optic neuropathy (AION), and in those with papilledema.[7] These studies led us to consider whether stress and strain on the ONH induced by ocular ductions may be a factor in the progressive loss of visual field and vascular complications of ONHD. Our goals were to determine if ocular ductions deform intrapapillary and peripapillary tissues in patients with ONHD using shape analysis and strain tracking techniques, to compare these deformations with previously published data in healthy persons and patients with other optic neuropathies, and to consider the role of gaze-evoked strains in the evolution and complications of ONHD.

https://doi.org/10.1016/j.ophtha.2017.12.006
ISSN 0161-6420/17

Methods

Inclusion Criteria

The diagnosis of ONHD was based on the typical ophthalmoscopic features that included visible intrapapillary deposits in most cases, sometimes associated with elevation of the optic disc; vascular anomalies; and peripapillary retinal pigment epithelial changes. Regardless of whether drusen were visible or buried, all patients underwent a B-scan or fundus autofluorescence photography that confirmed the diagnosis. All patients demonstrated OCT findings consistent with the diagnostic criteria defined by the Optic Disc Drusen Studies Consortium recommendations.[10] We excluded any patient with a coexistent disc anomaly (e.g., pseudopapilledema without drusen, tilted optic disc, high myopia, staphylomas, or otherwise dysplastic conditions), optic neuropathies, or papilledema. This study was approved and complied with policies of the State University of New York Stony Brook Committee on Research Involving Humans and complied with the tenets of the Declaration of Helsinki and the Health Insurance Portability and Accountability Act.

Image Acquisition

A Cirrus 5000 SD-OCT device (Carl Zeiss Meditec, Inc., Dublin, CA) was used to acquire (1) a 200 × 200 optic disc cube and (2) a 5-line, high-definition axial raster (9 mm in length at 0.125-mm intervals) with a signal strength of 7 or more. The optic disc cube was used to calculate the mean retinal nerve fiber layer thickness. The Cirrus 5000 SD-OCT produces vertically stretched raster images with an aspect ratio of 3:2 (750 × 500 pixels; Fig 1). We corrected the aspect ratio from 3:2 to an unstretched aspect ratio of 9:2 (750 × 167 pixels) for shape analysis. To illustrate small differences, some of the figures are displayed in a stretched or 3:2 aspect ratio where indicated.

High-definition 5-line axial rasters were obtained in 2 head positions with the eyes in adduction and abduction to the extent that the patient and the fixed camera device would permit. Adduction was limited by the patient's nose against the lens element of the device at approximately 10° to 15° and abduction was less restricted at approximately 30° to 40°. These ranges were based on rotational head positions while the patient viewed the OCT fixation target using a head-mounted protractor. Scanning laser ophthalmoscopic image stabilization (FastTrac; Carl Zeiss Meditec, Inc, Dublin, CA) was used to register images. We used the most centrally positioned raster of the 5 raster lines in adduction as a baseline reference to compare with the axial raster obtained in abduction at the same location (Tracked to Prior option). Images were mirrored horizontally when necessary to align the temporal and nasal regions.

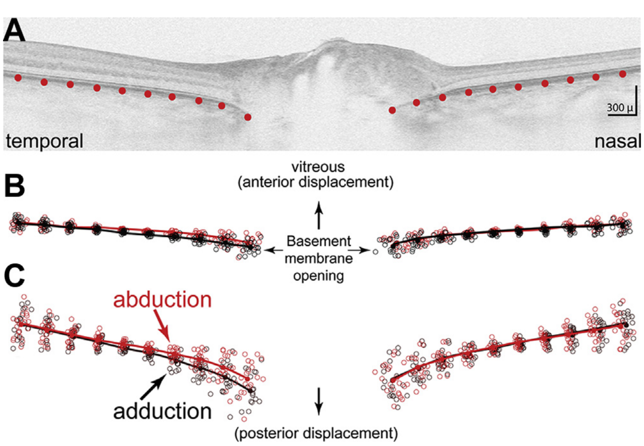

Figure 1. **A**, Diagram showing placement of 10 equidistant semilandmarks spanning 2500 μm on both sides of the basement membrane opening. **B**, Scatterplot showing semilandmarks from each participant in abduction (*red circles*) and adduction (*black circles*) after normalizing for location, size, and rotation (Procrustes superimposition). The lines show the mean (consensus) shapes for each group (*black* for adduction, *red* for abduction). **C**, Three-fold vertically stretched image illustrating differences in more detail. Overall, the shape in adduction is posteriorly displaced temporally relative to the nasal side compared with abduction, which is displaced more anteriorly. The difference in shapes between abduction and adduction was statistically significant ($P < 0.01$).

Geometric Morphometric Shape Analysis

We used geometric morphometrics to analyze the shape of the peripapillary basement membrane (ppBM) layer imaged on the spectral-domain OCT raster. This is a well-established method that quantifies and analyzes shape and its covariation with other variables.[11−14] The methodologies are detailed in a primer by Zelditch et al.[14] Additional references and software can be found online at http://life.bio.sunysb.edu/morph.[13] The application of this technique to the analysis of the ONH has been described in several previous publications.[7,15−17] The tps software[13] was used in this analysis. A brief description follows.

Geometric morphometrics define shape as that geometric property that remains after normalizing for differences in centroid location, scale, and rotation. Shapes are defined by a series of landmarks whose coordinates are treated as row vectors. Each shape vector can be represented as a distance-based variable, at a single location in a multidimensional space that can be analyzed statistically.

Regarding digitizing semilandmarks, we superimposed a 2500-μm rectilinear grid on the temporal and nasal side of the basement membrane opening (BMO) of a 9-mm axial raster image (unstretched [9:2] aspect ratio) using imaging software (Photoshop; Adobe Systems, San Jose, CA). The grid was used to position 10 equidistant semilandmarks (defined as landmarks placed along a curve or surface) spanning a distance of 2500 μm from the edge of the basement membrane layer on both sides of the BMO. Each semilandmark was positioned along the outer edge of the ppBM layer starting at the edge of the BMO (Fig 1A). Semilandmark placement was performed on image files that were de-identified with respect to name and eye position.

Generalized Procrustes analysis or Procrustes superimposition is a normalization process of superimposing all of the specimen shapes onto a mean shape in 3 sequential steps: first by translating the centroid of the semilandmarks to a single point of origin, then rescaling to a uniform size, and finally minimizing rotational differences between corresponding landmarks.

The thin plate spline displays differences in shape as a smooth deformation using an algorithm that interpolates differences between landmarks and can be visualized using vectors at each landmark. The thin plate spline also defines a set of shape variables (partial warps) that capture the differences between shapes. The partial warp scores generate data matrices that can be analyzed with the proper degrees of freedom using multivariate statistical methods.

Principal component analysis is used to identify and ordinate the variation in shape along a series of components that are linear combinations of the partial warps. In effect, principal component analysis identifies the important patterns of shape based on variance to determine if they distinguish patient groups (in this case, shape differences between abduction and adduction). The relative contribution of each principal component is expressed as a percent of the total variance. Principal component analysis was performed using a variance−covariance matrix of the shape variables.